10th Biennial International Conference & Exposition

P 032

An Efficient 3D Elastic Full Waveform Inversion of Time-Lapse seismic data using Grid Injection Method

Dmitry Borisov *(IPG Paris)* ***and Satish C. Singh**** *(IPG Paris)*

Summary

Full waveform inversion (FWI) is a powerful tool to quantify Earth properties of the subsurface from seismic data, and has become a major area of research. Because of very high computational cost, FWI has so far been used for either 2D full elastic or 3D acoustic media. However the Earth is three-dimensional, elastic and highly heterogeneous, and therefore, one would require a full 3D elastic wave equation for accurate modeling of amplitudes within inversion process. Acoustic approximation could impact significantly on the final inversion results due to the amplitude variation with offset (AVO) effect. Here we propose an efficient way to perform 3D elastic FWI for time-lapse seismic data using grid injection method, which allows for efficient calculation of synthetic seismograms after model alterations within a localized area. The technique allows for significant reductions in computational time and memory requirements without any significant loss in accuracy.

Keywords: *Numerical solutions; Wave propagation; Inverse theory*

Introduction

Full waveform inversion (FWI) is a powerful tool to determine quantitative images of the earth sub-surface from seismic data. The idea is based on minimizing the difference between observed and modeled data using an adjoint state technique (Tarantola, 1984). Compared to conventional methods, FWI allows to take into account the full information contained in seismic data. Because of very high computational cost, it has been used for either 2D full elastic media (Sears et al., 2010) or 3D acoustic (Plessix, 2009). It has also found applications in reservoir monitoring (Queisser and Singh, 2010) and pore pressure estimation (Roberts et al., 2008). However, the Earth is three-dimensional, elastic and highly heterogeneous, and therefore, one would require a full 3D elastic inversion. The extension to the elastic case with realistic model size is still a challenging task even on current computer architecture.

Here, we first present our implementation of 3D elastic FWI using multi- component, ocean-bottom cable seismic data in the context of marine environment. In our study heavily parallelized 3D wave propagation engine allows for an accurate modelling of the full wavefield in isotropic medium. The inversion stated as a local optimization problem and solved using iterative conjugate gradient method. Both the forward modelling part and the inversion part are performed in the time domain. We present successful application of the technique on part of a 3D SEG/EAGE overthrust model with a checkerboard test, demonstrating the feasibility to invert and quantify both P-and S-wave velocities. Being an important motivation factor in our study, these elastic parameters could bring valuable information about fluid content and could be used as a lithology indicator.

We further propose an efficient way to perform 3D elastic FWI of Time-Lapse seismic data using Grid Injection Method (Robertsson and Chapman, 2000). The Grid Injection Method (GIM) allows for an efficient calculation of synthetic seismograms after model alterations in a localized region where changes occur only inside a reservoir and hence is well suited for time-lapse seismic. The method is based on the principles of superposition and continuity of wavefields along a boundary and requires only calculations in the sub-volume and its neighborhood. This technique allows for significant reductions in computational time and memory requirements. A prototype of the GIM inversion for 2D media was introduced by Royale (2010), and here we present a 3D implementation of the grid injection method

Office 364, 1 rue Jussieu, 75238 Paris, France;
singh@ipgp.fr

for full elastic media, which has potential for time-lapse monitoring.

3D elastic Full Waveform Inversion

The goal of inversion is to determine detailed P and S-wave velocity models by fitting synthetically calculated seismic data with observed data. The FWI can be divided in two parts: forward problem and inverse problem. Forward modeling of seismic wavefield involves simulating wave propagation through the earth. We consider the 3D elastic wave equation in the first-order velocity-stress formulation:

$$\rho \partial_t \upsilon = \nabla \cdot c,$$

$$\partial_t \sigma = c : \nabla \upsilon,$$

where υ is the velocity vector, s the stress tensor, ρ the density, c the elastic tensor and " : " denotes the Frobenius inner product. This coupled system of equations is solved using Finite-Difference (FD) scheme with staggered grid, 2nd order in time and 4th order in space, e.g. O(Δt) (Levander,1988). Un-split convolutional perfectly matched layers (C-PML) are used to efficiently absorb undesirable reflections from model boundaries (Komatitsch and Martin, 2007). The algorithm is heavily parallelized using classical domain decomposition, allowing efficient and fast calculation of the 3D wavefield.

The inversion is stated as an optimization problem, which is solved using steepest-descent method. The algorithm is driven by iteratively minimizing the difference between the synthetic and the observed data in the least-square sense:

$$s = \sum_{shots} \int_0^T dt \sum_{recs} \left[d_{syn} - d_{obs} \right]^2,$$

where s is misfit, d_{syn} is the synthetic data and d_{obs} is the observed data. We have implemente inversion in the time domain and the algorithm enables the simultaneous inversion of both P- and S- wave velocities. To improve the current model, a steepest descent method with a conjugate gradient is used. At each iteration and for each shot, cross- correlation of the forward modeled wavefield and back- propagated residuals allows to determine the gradient for the Lamé parameters ($d\lambda$, $d\mu$). As Lamé parameters are poorly resolved, these values are converted to the gradient for P-wave and S-wave velocities (δVp, δVs) (Mora, 1987).
The model m is updated using

$$m_{n+1} = m_n - \alpha_n \gamma_n$$

where γ is a conditioned gradient direction and a is an optimal step-length at iteration n, calculated with a linear assumption (Pica et al., 1990).

For validation of the algorithm the inversion was tested on a part of the 3D SEG/EAGE overthrust model. The model dimensions are 6.4 km × 6.4 km × 1.6 km and the total number of grid points is about $8.2*10^6$. One hundred and eleven sources (11 × 11) spaced at 500 m were used to generate synthetic data. The source was a Ricker wavelet

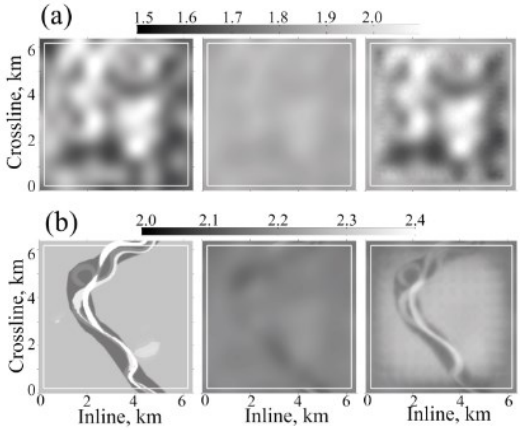

Figure 1: The results of 3D elastic FWI on a part of SEG/EAGE overthrust model. Horizontal slices for S-wave velocity at 0.7 km (a) and at 1 km depths (b) respectively. The true (left), starting (middle) and inverted models (right) are shown. The results for P-wave velocity have shown similar behavior and thus were omitted.

with a dominant frequency of 7 Hz. 19821 (141 × 141) receivers regularly spaced at 40 m interval were placed close to the surface. Each receiver measured three velocity components. To demonstrate the efficiency of the inversion, we show a depth slice though the model in Figure 1. The inversion results show good recovery of main features for both P- and S-wave velocities. The channel (Figure 1b) is accurately recovered as well as the background velocity in the upper layers (Figure 1a).

Grid Injection Method

The Grid Injection Method (GIM) allows the re-calculation of the seismic response over a specific subdomain through the insertion of the wavefield inside a Finite Difference (FD) grid, without re-calculating the wavefield in the whole model space. A source field can be introduced into a localized FD grid by injecting an analytical source solution along a closed surface (Alterman and Karal, 1968). Similarly, the wavefield recorded along a closed surface can be used as a source

wavefield to compute the wavefield within the injected grid region. Figure 2 illustrates the basic idea of the method. The region where the model is altered (e.g. oil/gas reservoir, injected CO2) is referred to as injection subvolume, *Vi*. The injection surface *Si* encloses this altered region. The submesh *Ve* and associated surface *Se* surrounding sub-volume *Vi* are used to limit the part of the initial model where seismic wavefield is recomputed. The main idea of wavefield injection is to satisfy the principles of superposition and wavefield continuity across injection surface *Si*, while surface *Se* acts as an absorbing boundary.

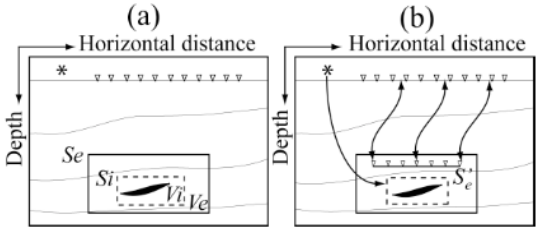

Figure 2: Schematic diagram showing the basic concept of the Grid Injection Method (Robertsson and Chapman, 2000). Initial model with source & receivers placed at the surface (a), and new source & receivers position close to the reservoir (b).

The method is demonstrated on a time-lapse example using a horizontal P-wave velocity model (Figure 3a) with a 3D ellipsoidal velocity perturbation in the center (Figure 3b). Figure 4 illustrates recalculation of the wavefield before and after model perturbations along a 2D slice going through the middle of the model. A snapshot of the wavefield after 2.1 s obtained from the full FD-simulation on the initial model is shown in Figure 4b. During the full modeling the wavefields at each time step are stored along injection surface *Si*. By injecting this wavefield, the response inside the submesh *Ve* is calculated on the initial and perturbed models. If the injection volume contains the initial model (Figure 4c), then the wavefield inside *Ve* would be equal to zero (Figure 4d). While for the perturbed model (Figure 4e) the wavefield inside *Ve* corresponds to the difference between initial and perturbed wavefield (Figure 4f). To obtain updated seismograms on the surface, the residual wavefield from some recording array *S'e* can be extrapolated to the surface receiver positions using Green's Function and added to the initial response. Obviously FD-calculation inside subvolume *Ve* is significantly faster than computing wavefield in the full volume.

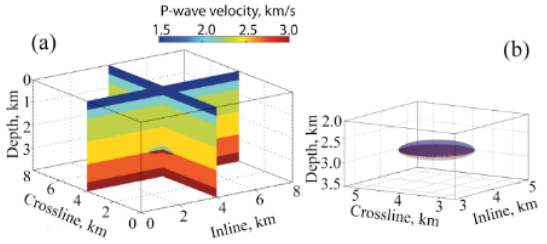

Figure 3: Initial 3D volume of P-wave velocity (a) and zoom on the model perturbation (b).

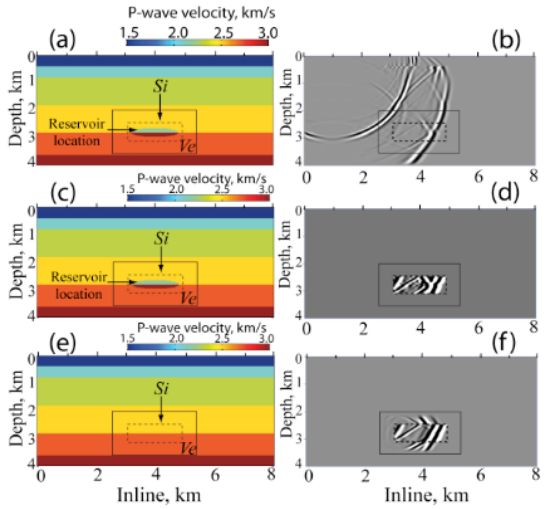

Figure 4: Wavefield recalculation using Grid Injection Method. (a), (c) & (e): vertical slices of P-wave velocity through the middle of the model. (b), (d), (f): corresponding snapshots of normal stress at 2.1 s. (b): the snapshot was calculated on the whole initial model. (d), (f): the snapshots were calculated on the part of the initial and perturbed models respectively, after wavefield injection across the surface *Si*.

Full Waveform Inversion using Grid Injection Method

We have integrated efficient forward modeling engine (cf. upper text) within 3D elastic FWI algorithm for time-lapse data in order to speed-up the inversion. To demonstrate the efficiency of the algorithm, the method is applied to the 3D elastic model with a lens-body perturbation, which is included for baseline model and completely removed for time-lapse model (Figure 3). To simplify the experiment we initially placed all receivers at some datum-level close to the zone of interest (Figure 2, surface S'e). This was done in order to calculate directly the difference between observed and modeled data inside the subvolume Ve, thus avoiding the extrapolation step. The corresponding geometry however can represent a real situation, e.g. a deep horizontal well or a VSP survey (vertical seismic profile). The data

observed on the surface can also be propagated to some depth assuming that the velocity model is well constrained for a baseline survey. The redatuming of the observed data will not significantly increase the total computational time as it would be done only once before the first inversion iteration.

The dimensions of the model are 8 km × 8 km × 4 km and the total number of grid points is about 32*10. The velocity perturbation is placed at 2.8 km depth and consists of two lens bodies with anomaly of an ±0.4 km/s and ±0.2 km/s for P- & S-waves, respectively. The experiment contains 49 sources with a Ricker wavelet of dominant frequency at 7 Hz with sparse spacing of 1 km, while the distance between receivers is 40 m in both horizontal directions. The results of 3D Elastic FWI on the whole model using in parallel 1024 processor cores are shown in Figure 5. Using GIM in the FWI, the inversion results were achieved on a desktop computer with only 8 processor cores and showed good recovery of main features for both P- & S-wave velocities (Figure 6). The 4D perturbation was accurately recovered and the total misfit was reduced by 95% after 30 iterations (Figure 7, 8). We are presently applying this algorithm to 3D surface seismic data.

Table 1 shows the comparison of the computational parameters for two cases: FWI using surface survey within the whole model and FWI using GIM. By reducing the model space, we sped up the computation by a factor of 20, while memory requirements (RAM) were reduced by a factor of 25. Only the memory storage on a hard disk was increased from 300 Gb to 600 Gb in order to keep the data, which was used for wavefield injection. However this does not represent a critical issue as this disk space is quite cheap and affordable nowadays.

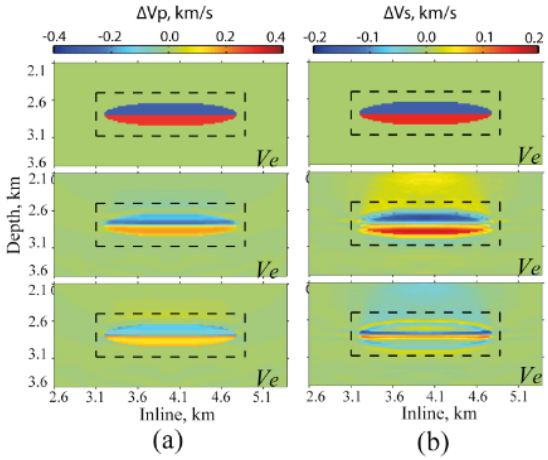

Figure 5: The results of 3D elastic FWI calculated on the whole model with a surface survey. Zoom on time-lapse velocity perturbation along vertical slices of P-wave (a) and S-wave (b): true (top), recovered (middle) and residual (bottom) velocity perturbations.

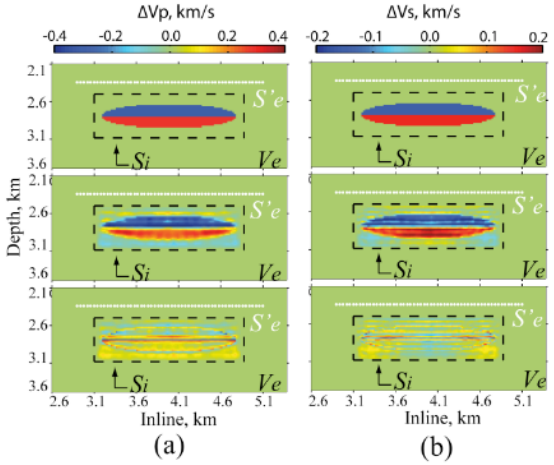

Figure 6: The results of 3D elastic FWI, accelerated by Grid Injection Method. Zoom on FD-submesh with time-lapse velocity perturbation along vertical slices of P-wave (a) and S-wave (b):true (top), recovered (middle) and residual (bottom) velocity perturbations. Receivers were placed on white dotted line (S').

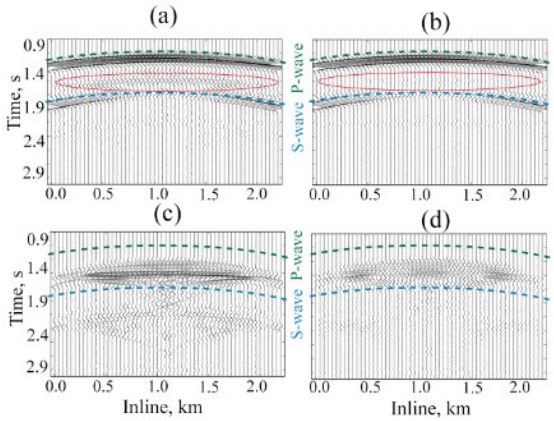

Figure 7: Vertical velocity recorded at receiver's position in localized FWI: (a) - before perturbations; (b) - after perturbations; (c) - the difference between (a) & (b); (d) – final FWI residuals after 30 iterations; (c) & (d) are shown on the scale increased 5 times in comparison with (a) & (b).

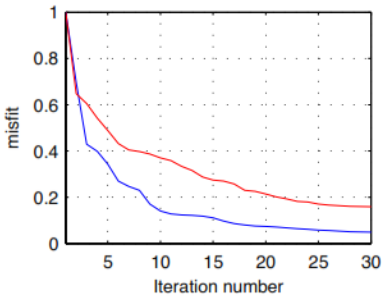

Figure 8: Comparison of misfit reduction for the FWI on the whole model with a surface survey (red line) and localized FWI (blue line).

	Conventional FWI (1)	Localized FWI (2)	(1) / (2)
CPU time (hours)	≈ 18000 (h)	≈ 900 (h)	≈ 20 (speed-up)
RAM, random-access memory (Gb)	≈ 810	≈ 33	≈ 25
Memory storage (Gb)	≈ 300	≈ 600	≈ 0.5

Table 1: Comparison of the computation parameters between FWI on the whole model with a surface survey and localized FWI.

Conclusions

We have developed a 3D elastic Full Waveform Inversion scheme in the time domain and successfully applied it to the complex synthetic example. Our algorithm shows good recovery of both P- and S-wave velocities and confirms the feasibility of 3D elastic FWI. However this technique is still prohibitively expensive in computation and thus requires high performance calculation architecture.

To increase the efficiency, we have also integrated Grid Injection Method within the inversion algorithm and compared the results from the FWI on the whole model and GIM based FWI for synthetic Time-Lapse datasets. The computational time was reduced by a factor of 20. Memory requirements (RAM) were reduced by a factor of 25. These significant decreases in computation and memory requirements enable to perform all calculations on a desktop with only 8 processor cores instead of using computer cluster with large number of processors. The proposed algorithm shows good recovery of velocity perturbations at reservoir level in time-lapse mode and shows big potential to the real datasets.

Acknowledgments

We thank LITHOS consortium for founding this project. We are also very grateful to Gillian Royle from CGG for 2D prototype and fruitful discussions. A significant part of the calculations in this work was performed on the local cluster at the Paris Institute of Earth science (IPGP) and at the French CEA scientific computing complex on TGCC Curie supercomputer.

References

Alterman, Z.S., and F.C. Karal, 1968, Propagation of elastic waves in layered media by finite-difference methods: Bulletin of the Seismological Society of America, 58, 367-398.

Komatitsch, D. and R. Martin, 2007, An un-split convolutional perfectly matched layer improved at grazing incidence for the seismic wave equation: Geophysics, 72, no. 5, 155-167.

Lavander, A., 1988, Fourth-order finite difference P-SV seismograms: Geophysics, 53, 1425-1436.

Mora, P., 1987, Nonlinear two-dimensional elastic inversion of multioffset seismic data: Geophysics, 52, 1211-1228.

Pica, A., J.P. Diet, A. Tarantola, 1990, Nonlinear inversion of seismic reflection data in a laterally invariant medium: Geophysics, 55, 284-292.

Plessix, R.-E., 2009, Three-dimensional frequency-domain full-waveform inversion with an iterative solver: Geophysics, 74, no. 6, WCC149–WCC157.

Quisser, M., and S.C. Singh, 2010, Time lapse seismic monitoring of CO2 sequestration at Sleipner using time domain 2D full waveform inversion: 80th Annual International Meeting, SEG, Expanded Abstracts, 28752879.

Roberts, M.A., S.C. Singh, and B.E. Hornby, 2008, Investigation into the use of 2D elastic waveform inversion from look-ahead walk-away VSP surveys: Geophysical Prospecting, 56, 883-895.

Robertsson, J.A.O., and C.H. Chapman, 2000, An efficient method for calculating finite-difference

seismograms after model alterations: Geophysics, 65, 907-918.

Royle, G.T. and S.C. Singh, 2010, Time-lapse Elastic Full Waveform Inversion using Injected Grid Method: 72nd Conference and Exhibition, EAGE, Extended Abstracts, A023.

Sears, T. J., P. J. Barton, and S. C. Singh, 2010, Elastic full waveform inversion of multicomponent ocean-bottom cable seismic data: Application to Alba Field, U. K. North Sea: Geophysics, 75, no. 6, R109–R119.

Tarantola, A., 1984, Inversion of seismic reflection data in the acoustic approximation: Geophysics, 49, 1259-1266.